Toxicology and Applied Pharmacology **157,** 203–212 (1999)
Article ID taap.1999.8685, available online at http://www.idealibrary.com on IDEAL®

# Induction of the Cell Cycle Regulatory Gene p21 (Waf1, Cip1) Following Methylmercury Exposure *in Vitro* and *in Vivo*[1]

Ying C. Ou,* Sally A. Thompson,* Rafael A. Ponce,*,† Jesara Schroeder,*
Terrance J. Kavanagh,*,† and Elaine M. Faustman*,†,‡,[2]

**Department of Environmental Health, University of Washington, Seattle, Washington 98195; †Center for Ecogenetics and Environmental Health and Institute for Risk Analysis and Risk Communication, Seattle, Washington 98195; and ‡Center on Human Development and Disability, Seattle, Washington 98915*

Received September 21, 1998; accepted April 6, 1999

**Induction of the Cell Cycle Regulatory Gene p21 (Waf1, Cip1) Following Methylmercury Exposure** *in Vitro* **and** *in Vivo.* **Ou, Y. C., Thompson, S. A., Ponce, R. A., Schroeder, J. L., Kavanagh, T. J., and Faustman, E. M. (1999).** *Toxicol. Appl. Pharmacol.* **157, 203–212.**

**Methylmercury (MeHg) is recognized as a significant environmental hazard, particularly to the development of the nervous system. To study the molecular mechanisms underlying cell cycle inhibition by MeHg, we assessed the involvement of p21 (Waf1, Cip1), a cell cycle regulatory gene implicated in the $G_1$ and $G_2$ phases of cell cycle arrest, in primary embryonic cells and adult mice following MeHg exposure. Previous literature has supported the association of increased p21 expression with chondrocyte differentiation. In support of this finding, we observed an increasing p21 expression during limb bud (LB), but not midbrain central nervous system (CNS) cell differentiation. Both embryonic LB and CNS cells responded to MeHg exposure with a concentration-dependent increase in p21 mRNA. In the parallel adult study, C57BL/6 female mice were chronically exposed to 10 ppm MeHg via drinking water for 4 weeks. While there was limited or absent induction of Gadd45, Gadd153, and the γ-glutamylcysteine synthetase catalytic subunit, p21 was markedly induced in the brain, kidney, and liver tissues in most of the animals that showed MeHg-induced behavioral toxicity such as hyperactivity and tremor. Furthermore, the induction of p21 mRNA was accompanied by an increase in p21 protein level. The results indicate that the activation of cell cycle regulatory genes may be one mechanism by which MeHg interferes with the cell cycle in adult and developing organisms. Continued examination of the molecular mechanisms underlying cell cycle inhibition may potentially lead to utilization of this mechanistic information to characterize the effects of MeHg exposure** *in vivo.* 

*Key Words:* **methylmercury; p21 (Waf1, Cip1); cell cycle.**

Methylmercury (MeHg)[3] is recognized as a significant environmental hazard, particularly to the development of the nervous system. While the poisoning episodes in Japan in the 1950s and Iraq in the 1970s have led us to recognize the myriad health effects associated with MeHg exposure, the potential developmental effects associated with prolonged low level MeHg exposure, such as through maternal ingestion of seafood, remain uncertain. One of the main obstacles to assessing the risk associated with low level MeHg exposure comes from our inability to identify critical early events that lead to toxicity and that occur before the onset of neurobehavioral changes.

To understand the effect of MeHg on the CNS, several studies have attempted to characterize histopathological changes, which may manifest as neurobehavioral alterations. Following *in utero* exposure to high or moderate doses of MeHg, neuronal displacement and loss in the fetal brain is observed upon histological examination (Choi *et al.*, 1978; Harada *et al.*, 1977). However, the identification of similar structural changes associated with lower doses of MeHg exposure, a more common human exposure profile, often fails (Lapham *et al.*, 1995). With high doses of MeHg exposure, alterations in both neuroblast proliferation and neuronal migration are implicated in the observed histological changes (Clarkson, 1991). The effects of lower doses may also involve similar alterations in cell cycling and cell migration, which may be too subtle to detect upon gross histological examination. Therefore, to identify more subtle changes presumably associated with lower doses of MeHg exposure, one approach may lie in the identification of molecules that are involved in cell cycling or cell migration and are responsive to MeHg.

We have studied the molecular mechanism underlying the cell cycle alteration by MeHg for several reasons. First, avail-

[1] Presented in part at the Society of Toxicology Meeting, Anaheim, California, March, 1996.

[2] To whom correspondence should be addressed at the Department of Environmental Health, Roosevelt, Suite 100, 4225 Roosevelt Way NE, University of Washington, Seattle, WA 98105. Fax: (206) 685-4696; E-mail: faustman@u.washington.edu.

[3] Abbreviations used: ANOVA, analysis of variance; BrdU, 5-bromo-2′-deoxyuridine; Cdks, cyclin-dependent kinase; CNS, midbrain central nervous system; DEM, diethylmaleate; EB, ethidium bromide; Gadd genes, growth arrest and DNA damage responsive genes; GCS-HC, γ-glutamyl cysteine synthetase heavy chain subunit; Hoechst, Hoechst 33258; LB, limb bud; MAP, mitogen-activated protein; MeHg, methylmercury; PCNA, proliferating cell nuclear antigen; RB, retinoblastoma; SAPK, stress-activated protein kinase.



0041-008X/99 $30.00

able evidence from studies using human autopsy samples, animal tissues, and cells exposed *in vitro* demonstrate that impaired cell proliferation is a consistent and sensitive end point of MeHg toxicity (Howard and Mottet, 1986; Miura and Imura, 1987; Ponce *et al.,* 1994; Rodier *et al.,* 1984; Sager, 1988; Vogel *et al.,* 1986). Second, because normal development requires precisely timed cellular proliferation and differentiation, perturbation of the cell cycle could potentially explain the multiple toxic effects of MeHg on the developing CNS. Moreover, neuronal proliferation and migration are necessarily coregulated to ensure proper development (Chae *et al.,* 1997; Nakayma *et al.,* 1996; Takahashi *et al.,* 1996). Finally, understanding the molecular mechanism underlying the cell cycle alteration by MeHg may potentially lead to the identification of markers for studying effects associated with low doses of MeHg exposure *in vivo.*

Activation of signal transduction pathways with subsequent induction of cell cycle regulatory genes has been proposed as one potential mechanism underlying cell cycle arrest resulting from environmental insults. Among those cell cycle regulatory genes identified to date are the tumor suppressor proteins p53, p21 (Waf1, Cip1), Gadd153, and Gadd45. Distinct signal transduction pathways leading to induction of Gadd genes and p21 have clearly been identified in response to specific types of injuries. For example, the cytotoxic agents taxol and cisplatin can each induce cell cycle arrest via the induction of Gadd153, but only cisplatin exerts this effect via the activation of tyrosine protein kinase pathways (Gately *et al.,* 1996). Further, Gadd genes and p21 can each be activated by a variety of extracellular signals that modify cellular thiol-redox status and increase intracellular calcium levels (Bartlett *et al.,* 1992; Chen *et al.,* 1992; Fornace *et al.,* 1989; Russo *et al.,* 1995). However, oxidative stress resulting from DEM exposure induces expression of p21, but not Gadd45 (Russo *et al.,* 1995). Finally, DNA damage-induced p21 expression occurs via a p53-dependent pathway (el Diery *et al.,* 1993), while expression of p21 induced by oxidative stress is p53-independent (Russo *et al.,* 1995). Similarities in effects on calcium homeostasis (Hare *et al.,* 1993) and oxidative stress (Yee and Choi, 1994) between many of these agents and MeHg suggest that MeHg-induced cell cycle alterations may also involve the activation of specific signaling pathways resulting in the induction of cell cycle regulatory gene expression.

The cell cycle regulatory gene p21 was originally discovered as a prime mediator for p53-induced $G_1$ arrest following DNA damage (el Deiry *et al.,* 1993). p21 is a negative regulator of several cdks that are each involved in the progression of different cell cycle phases (Xiang *et al.,* 1996). By inhibiting the activity of $G_1$ cdks, p21 is believed to inhibit the cell cycle transition at the $G_1$–S margin by blocking RB protein phosphorylation (Harper *et al.,* 1993). In addition to its role in the $G_1$ transition, p21 also inhibits DNA replication in the S phase by suppressing the ability of the PCNA to activate DNA polymerase $\sigma$ (Waga *et al.,* 1994). More recently, emerging evidence has also supported the role for p21 in control of the $G_2$–M transition (Waldman *et al.,* 1996), cell senescence, and terminal differentiation (Parker *et al.,* 1995).

We hypothesize that MeHg-induced alteration of calcium homeostasis and oxidative stress can activate a distinct signal transduction pathway, leading to the observed cell cycle alteration. To test this hypothesis, our first step is to identify the target cell mediators. We have previously shown that the activation of Gadd45 and Gadd153 (Ou *et al.,* 1997) is associated with the dose-dependent alteration of cell cycling in primary embryonic CNS cells *in vitro* (Ponce *et al.,* 1994). The present study examines whether another cell cycle mediator, p21, participates in the cell cycle alterations induced by MeHg. In addition, to determine whether the induction of cell cycle regulatory genes such as p21 occurs *in vivo,* an initial investigation in adult mice following chronic low dose MeHg exposure is presented. The study here provides further evidence that induction of cell cycle regulatory genes may underlie the cell cycle changes induced by MeHg exposure.

## METHODS

***Cell culture.*** Primary micromass cultures were prepared according to the procedure described by Flint (1983) and modified by Ribeiro and Faustman (1990). Briefly, gravid uteri were removed from pregnant (12.5 day postcoitum) Sprague–Dawley rats (Bantam and Kingman Universal, WA). Embryonic midbrain CNS and limb bud (LB) cells were dissected and dissociated into single cell suspensions and plated as 10-$\mu$l aliquots at a concentration of $5 \times 10^6$ cells/ml for CNS and $2 \times 10^7$ cells/ml for LB. Ham's F-12 medium containing 10% fetal bovine serum, 50 U/ml penicillin, 5 mg/ml streptomycin, and 5.8 mg/ml L-glutamine was added to the cultures after a 2-h attachment period. The dishes were then incubated at 37°C with 95% air/5% $CO_2$ and 100% humidity for 5 days. All cell culture reagents were purchased from GIBCO Life Technology Inc. (Grand Island, NY).

***Chemical treatments.*** The stock solution of methylmercury(II) hydroxide (1 M) (Alfa Aesar, Ward Hill, MA) was prepared as 1 mM in water. A final concentration of MeHg was further diluted in water and then applied in the culture medium to Day 1 cultures (24-h postplating). Colchicine (Sigma, St. Louis, MO) stock solution was prepared in water and further diluted in culture medium. CNS and LB cells were cultured in a Plexiglass chamber with 95% air/5% $CO_2$ and 100% humidity and placed in an incubator at 37°C (Ponce *et al.,* 1994). Cytotoxicity and differentiation were assessed 24 and 48 h after MeHg and colchicine treatments and on Day 5 cultures.

***Cytotoxicity and differentiation assessment.*** Cell viability was monitored by the uptake of neutral red on the basis that neutral red is only accumulated in lysosomes of viable cells (Whittaker and Faustman, 1992). CNS differentiation was assessed with hematoxylin staining, in which the intensity of staining is correlated with degree of neurite extension and neuronal differentiation (Whittaker *et al.,* 1994). Differentiation of LB cells was quantified by Alcian blue staining of sulfated proteoglycans, a marker that is expressed in differentiated LB cells (Whitaker and Faustman, 1992). The intensity of hematoxylin and Alcian blue staining was quantified by image analysis (American Innovision-videometric 150, San Diego, CA).

***Cell cycle analysis.*** Cell cycling rate was determined as the fraction of cells successfully reaching a new $G_0/G_1$ phase and was measured by BrdU (Sigma) and Hoechst (Sigma) analysis as previously described (Ormerod and Kubbies, 1992; Rabinovitch *et al.,* 1983). Cells that undergo DNA synthesis in the presence of BrdU substitute BrdU for thymidine. Accordingly, as BrdU quenches Hoechst fluorescence but not EB fluorescence, this substitution will

result in the appearance of a new cell population on an EB–Hoechst flow cytogram concomitant with a reduced fluorescence along the Hoechst axis (Ormerod and Kubbies, 1992; Rabinovitch *et al.,* 1983). In brief, BrdU, at a final concentration of 80 $\mu$M, was added to cultures in conjunction with MeHg treatments. At the end of exposure period, cells were harvested under sodium lamp illumination to avoid BrdU-induced photosensitization. The cell pellet was then suspended in 500 $\mu$l of 1.2 $\mu$g/ml Hoechst/10% DMSO (v/v; Sigma) and frozen at −80°C until all the time points were collected. Cells were thawed and placed in phosphate-buffered saline buffer containing 0.154 M NaCl, 0.1 M Tris, pH 7.4, 0.5 mM $MgCl_2$, 0.2% bovine serum albumin, 0.1% Nonidet-P40, 5.9 $\mu$g/ml Hoechst, and 3 $\mu$g/ml EB. Flow cytometry was performed using a 525 ± 18-nm bandpass filter for Hoechst emission and a 580-nm long pass filter for EB emission and analyzed according to the method of Ormerod and Kubbies (1992) using the software program MultiPlus (Phoenix Flow Systems).

***Animal treatments.*** Animal housing and exposure of MeHg for Studies A and B were conducted according to the procedures previously described (Ou *et al.,* 1997). In brief, C57BL/6 female mice 4 weeks of age were allowed to acclimate for 2 weeks prior to the beginning of the study and were arbitrarily placed into dose groups of 0, 3, or 10 ppm MeHg with methylmercury hydroxide administered in the drinking water for 4 weeks. Twice weekly animals were weighed, water was changed, and fluid consumption was recorded for the duration of the study. MeHg dosing solutions were verified as stated concentrations by cold vapor atomic absorption spectrophotometry (Dr. James Woods, University of Washington, Seattle, WA). During the study period, any abnormal neurobehaviors, including hyperactivity, scoliosis, placing deficits, posterior paresis, and tremor were recorded without knowledge of treatment history. At the end of the 4-week exposure period, tissues (brain, liver, and kidney) from control and MeHg-treated animals were dissected, quick-frozen immediately upon procurement, and stored at −80°C until RNA isolation. In Study B, in addition to the mRNA expression analysis, selected tissue and blood samples from control and 10-ppm treatment groups were collected for MeHg analysis by cold vapor atomic absorption spectrophotometry (Frontier Geosciences Inc., Seattle, WA).

***Northern blotting.*** Total RNA was isolated using Trizol Reagents (Gibco BRL, Grand Island, NY) according to the manufacturer's instructions. Fifteen micrograms of RNA was electrophoresed in a 1% formaldehyde agarose gel and transferred to a nylon membrane (GeneScreen Plus, DuPont NEN, Boston, MA) using the downward transfer method by Turboblotter (Schleicher and Schuell, Keene, NH). A $^{32}$P-labeled cDNA probe (1.2 kb Kpn I–Sac I fragment for p21) was prepared by a random priming method (Ambion, Austin, TX). The membrane was prehybridized for at least 1 h at 60°C in a hybridization buffer containing 100 $\mu$g/ml denatured salmon sperm DNA, 10% dextran sulfate, 1 M NaCl, and 1% SDS. The hybridization was then carried out in the same buffer with $4-8 \times 10^5$ cpm/ml [$^{32}$P]cDNA probe (60°C, overnight), followed by washing (2× SSC, 0.1% SDS; 1× SSC is 5 mM NaCl and 1 mM NaCitrate) at room temperature for 15 min and a high stringency wash (0.1× SSC, 0.1% SDS) at 60°C for 50 min. For detecting message levels of 18S rRNA, 10 ng rat/human 18S rRNA antisense probe, 5′-CACCTCTAGCG-GCGCAATAC-3′, was labeled by an end-labeling method using T4 kinase (Gibco BRL) at 37°C for 30 min. Hybridization was performed in a hybridization buffer containing 0.1% SDS, 100 $\mu$g/ml salmon sperm DNA, 5× Denhardt's (0.02% Ficoll, 0.02% polyvinylpyrrolidone 360, 0.2% bovine serum albumin), 6× SSPE (1.0 M NaCl, 60 $\mu$M $NaH_2PO4$, pH 7.4, 60 $\mu$M EDTA, pH 7.4) at 52°C for at least 6 h. The relative expression of p21 mRNA levels between control and MeHg-treated samples was determined by a densitometer (Scanmaster 3, Howtek, Hudson, NH) with subsequent normalization to the intensity of the 18S rRNA signal to ensure equal sample loading.

***Western blotting.*** Brain, kidney, and liver tissues were weighed and diced into small pieces. Approximately 100 mg of tissue was homogenized in 0.3 ml ice-cold RIPA buffer (10 mM Tris–HCl, pH 7.4, 150 mM NaCl, 1% NP40, 0.5% sodium deoxycholate, 0.1% SDS, 5 mM EDTA) with a cocktail of protease inhibitors (10 $\mu$g/ml PMSF, 2 $\mu$g/ml aprotinin, 5 $\mu$g/ml leupeptin, 1 $\mu$M pepstatin A, 100 $\mu$M benzamidine). Following incubation on ice for 30 min, the homogenates were centrifuged at 15,000*g* for 20 min at 4°C to obtain total cell lysates. Protein concentration was determined by the BCA method (Pierce, Rockford, IL). One hundred micrograms of protein per sample were separated by electrophoresis on a 12% SDS–PAGE gel for p21 protein detection. Protein samples were further transferred to Protran Nitrocellulose membranes (Schleicher and Schuell) followed by Ponceau S staining to verify equal sample loading and transfer. Western Blotting analysis of p21 protein was performed using enhanced chemiluminescence (Amersham Life Science, Arlington Heights, IL) with a purified rabbit polyclonal antibody against a peptide corresponding to amino acids 146–164 from the carboxyl terminus of human p21 (Santa Cruz Biotechnology, Santa Cruz, CA) and anti-rabbit IgG HRP-conjugated secondary antibody (Amersham Life Science).

***Immunoprecipitation.*** Briefly, cleared protein lysates were immunoprecipitated with a 5 $\mu$g p21 polyclonal rabbit antibody or an anti-rabbit IgG antibody (Santa Cruz Biotechnology) in RIPA buffer containing 0.1% BSA. Each sample was incubated with tilting for 1 h at 4°C, followed by an additional 2-h incubation at 4°C with 2.5 mg protein A–Sepharose (Pharmacia, Piscataway, NJ). The samples were then washed three times with RIPA buffer, followed by another wash with 10 mM Tris–HCl, pH 7.4, and separated by SDS–PAGE electrophoresis on a 12% gel. Immunoblotting was performed with a p21 polyclonal rabbit antibody (Santa Cruz Biotechnology) and enhanced chemiluminescence detection (Amersham Life Science).

***Statistical analyses.*** Levels of p21 mRNA expression among Days 1, 2, 3, and 5 of CNS and LB cultures were analyzed by ANOVA; when appropriate, post-hoc testing (Dunnett) was used to determine whether expression levels on Days, 2, 3, and 5 differ from those on Day 1 at $p = 0.05$ (Miller, 1981). Levels of p21, Gadd45, Gadd153, and GCS-HC mRNA expression among control and treatment groups were analyzed by ANOVA, and, when appropriate, post-hoc testing (Dunnett) was used to determine whether the treated groups differ from the controls at $p = 0.05$ (Miller, 1981). All analyses were performed by SYSTAT for Macintosh (SYSTAT, Inc., Evanston, IL).

## RESULTS

### *Developmental Expression of p21 mRNA in CNS and LB Cultures*

Primary CNS and LB cells were prepared from Gestation Day 12 embryos and cultured for 5 days. Primary embryonic CNS and LB cells undergo differentiation over the 5-day culture period *in vitro,* as indicated by the increasing expression of neuronal differentiation markers in CNS cells and of sulphated polysaccharides in LB cells (Whittaker *et al.,* 1994). Increased expression of p21 is associated with terminal differentiation of many cell types including myoblasts (Halevy *et al.,* 1995). We found a differential expression of p21 mRNA associated with differentiation in CNS and LB cultures. A gradual decrease in the expression of p21 mRNA from Days 1 to 5 in CNS cells was consistently observed, however these changes are not significantly different (Fig. 1). For example, scanning densitometry measurements from three separate experiments revealed that mRNA expression levels of p21 on Day 5 were 60 ± 12%, respectively, of those on Day 1 for CNS cells. In contrast, for LB cells, a marked increase in p21 expression from Days 1 to 5 was observed ($p < 0.05$). The average expression of p21 on Days 3 and 5 of LB cultures was 900 ± 230 and 580 ± 130%, respectively, of the expression levels on Day 1 (Fig. 1).

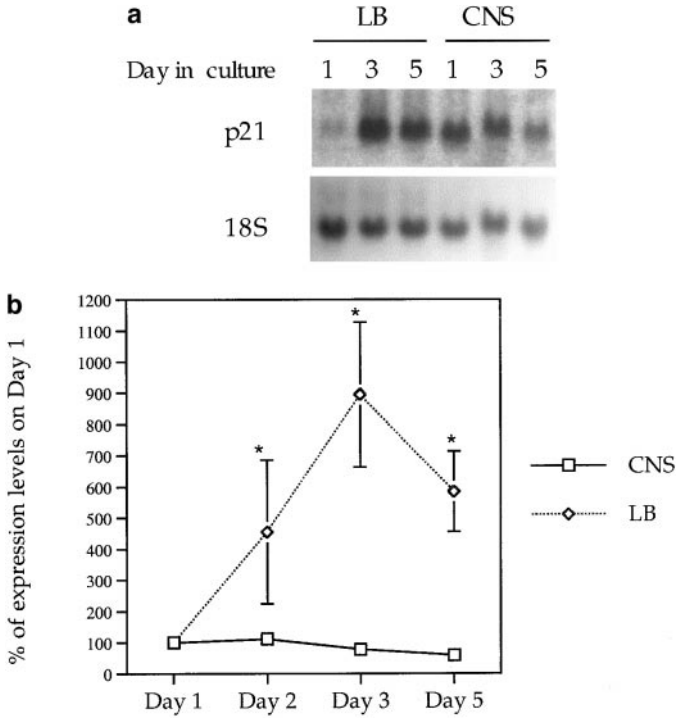


**FIG. 1.** Changes in p21 mRNA levels during differentiation of CNS and LB cells in cultures. Micromass primary CNS and LB cells were prepared and cultured for 5 days. Total RNA was isolated on Days 1, 2, 3, and 5 of the culture. Northern analysis was carried out as described in Methods and a representative blot is shown. Following hybridization with a $^{32}$P-labeled p21 cDNA probe, blots were stripped and reprobed with a $^{32}$P-labeled probe for 18S rRNA. (a) A representative blot showing differential expression of p21 during differentiation of CNS and LB cells in cultures. (b) Quantification of p21 relative mRNA levels during differentiation of CNS and LB cells in cultures. Northern blotting with subsequent densitometry scanning was used to quantify mRNA levels. The levels on Days 2, 3, and 5 are expressed relative to those on Day 1. Bars represent the means ± SEM of three independent experiments. When no error bars are observed, the SEM falls within the plot symbol. *Significantly different from the expression levels of Day 1 ($p < 0.05$).

### *Concentration-Dependent Decrease in Cell Viability and Cell Cycling Following MeHg Exposure*

The neutral red uptake assay is a measure of relative numbers of viable cells and therefore measures the combined effect of MeHg on both cell lethality and proliferation. Cell cycling rates were determined as the proportion of cells successfully completing a round of cell cycle, which can be measured by Brdu–Hoechst labeling followed by flow cytometric detection as previously described (Ormerod and Kubbies, 1992; Rabinovitch *et al.*, 1983). Following MeHg exposure for 24 and 48 h, a dose-dependent decrease in number of viable cells and cell cycling rates were observed, and alteration of cell cycling appeared to be a more sensitive end point compared to the decrease in viable cells (Table 1). For example, following 2 μM MeHg exposure for 24 and 48 h, the percentage of cells successfully completing one cell division was only 25 and 13%, respectively, of concurrent untreated controls, while the percentage of viable cells was 67 and 33% of respective controls. In these experiments, we also used the microtubule inhibitor colchicine as a positive control to delineate the relationship between effects of MeHg on cell viability and cell cycling. Following 2 μM MeHg treatment for 24 h, the number of viable cells was 67 ± 11% of control untreated cells. At similar levels of cytotoxicity, 25 nM of colchicine resulted in a more pronounced inhibition of cell cycling (99% inhibition) compared to MeHg-treated cells, which showed approximately 75% inhibition (Table 1). Following 2 μM MeHg treatment for 48 h, cell cycling rate declined to only 13% of untreated controls. Alternatively, at similar levels of cell cycle inhibition, MeHg appeared to be the more lethal agent; the survival of CNS cells was 33% of untreated controls in MeHg-treated cells compared to 46% of untreated controls in colchicine-treated cells at 48 h (Table 1).

### *Induction of p21 mRNA Expression in Primary Embryonic CNS and LB Cells Following MeHg Exposure*

We have previously demonstrated a dose-dependent induction of mRNA for the growth arrest genes Gadd45 and Gadd153 following MeHg exposure in primary CNS cells (Ou *et al.*, 1997). To further understand the mechanisms of cell cycle alteration in MeHg-exposed cells, we determined whether p21, another regulator involved in control of cell cycle arrest, can also be activated following MeHg exposure. On Day 1 of the cultures, corresponding to 24 h postplating, primary CNS and LB cells were treated with 1 or 2 μM MeHg for 24 h. Northern blotting and densitometric scanning of resultant autoradiographs were used to determine the relative mRNA expression in control and treated cells. As shown in Fig. 2, MeHg caused a dose-related induction of p21 mRNA in both CNS and LB cells. Compared to untreated controls, 2 μM MeHg exposure for 30 h causes a 215 ± 12% increase in the proportion of $G_2$–M phase cells with a corresponding decrease (40 ± 3%) in the S phase population (Ponce *et al.*, 1994). At this concentration, we observed an average increase in p21 mRNA expression of 2.0 ± 0.4-fold for CNS cells and 2.6 ± 0.5-fold for LB cells compared to untreated control cells (Table 2). The magnitude of p21 mRNA induction in MeHg-treated embryonic cells, however, is less profound than that of Gadd45 and Gadd153 (Ou *et al.*, 1997). For example, upon 2 μM MeHg exposure for 24 h, the fold induction of Gadd45 and Gadd153 is approximately 6.2 and 4.9 in CNS cells and 3.9 and 5.1 in LB cells, respectively. GCS-HC expression is induced following subchronic and chronic MeHg exposure in adult mouse brain and kidney (Li *et al.*, 1996; Woods and Ellis, 1995). We found that with 24 h MeHg exposure, the expression of GCS-HC mRNA levels was strongly induced in LB cells, but not in CNS cells (Table 2).

**TABLE 1**
**Dose–Response Relationship for Effects of MeHg Treatment on Cell Viability and Cell Cycling in Primary Embryonic CNS Cells**

| | 24-h treatment | | 48-h treatment | |
|---|---|---|---|---|
| | Cell viability | Cell cycling | Cell viability | Cell cycling |
| MeHg ($\mu$M) | | | | |
| 0 | 100 | 20.4 ± 3.8 (100) | 100 | 56.6 ± 5.9 (100) |
| 1 | 85.5 ± 6.1* | 13.2 ± 1.6* (64.7) | 60.7 ± 7.1* | 40.7 ± 3.9* (71.9) |
| 2 | 66.5 ± 11.2* | 5.0 ± 1.4* (24.5) | 33.1 ± 0.5* | 7.4 ± 2.1* (13.1) |
| 4 | 24.6 ± 12.2* | 0.0 ± 0.0* (0) | 4.8 ± 2.2* | 1.5 ± 1.2* (2.6) |
| Colchicine (nM) | | | | |
| 12.5 | 89.4 ± 8.9* | 17.5 ± 4.5* (84.5) | 80.4 ± 0.4* | 56.0 ± 17.0 (98.9) |
| 25 | 69.3 ± 7.8* | 0.25 ± 0.25* (1.2) | 46.3 ± 6.6* | 9.0 ± 0.0* (15.9) |

*Note.* CNS or LB cells were treated with 0, 1, or 2 $\mu$M MeHg for 24 or 48 h. Cell viability was determined by neutral red uptake and was expressed relative to control untreated cells. Cell cycling rate was expressed as the fraction of cells successfully completing one round of cell cycle, and determined by Brdu–Hoechst staining and flow cytometry. The value in parentheses indicates the percentage of response relative to control untreated cells. All the values are the means ± SEM from a least four independent experiments.

* Significantly different from control cells.

### *Induction of p21 mRNA Expression Following Chronic MeHg Exposure in the Adult Female Mouse*

In order to determine whether the induction of p21 by MeHg occurs *in vivo*, we conducted chronic MeHg exposure in developing embryos as well as in female adult mice. While the analysis of embryonic data is still in progress due to the need for a highly sensitive technique to measure gene expression in embryos, we report here the results from the adult study for comparison. Adult female mice were exposed to MeHg (3 or 10 ppm) in their drinking water for 4 weeks, an exposure level that was chosen to simulate a likely human exposure profile (Harada, 1977), and has been shown to cause developmental malformations in mice (Thompson, 1996). During the study period, body weight development and fluid consumption were recorded, and any abnormal neurobehaviors, including hyperactivity, scoliosis, placing deficits, posterior paresis, and tremor were recorded without prior knowledge of treatment history. In both studies, no significant differences in body weight development and fluid consumption between control and treatment groups were found.

*Study A.* At the end of 4-week exposure period, animals were examined for symptoms of toxicity and tissues were obtained for Northern blot analysis. Animals in the 3-ppm group did not reveal any overt toxicity or mRNA induction in any of the genes examined. In the 10-ppm group, three of five animals showed overt MeHg toxicity, including hyperactivity, scoliosis, placing deficits, posterior paresis, and tremor. Upon examination, none of the animals appeared to have any gross organ abnormalities. Interestingly, the induction of p21 mRNA expression was only observed in animals that showed signs of toxicity. An estimation of 6.8 ± 1.4, 12.9 ± 2.1, and 13.7 ± 0.3-fold increase in p21 mRNA was observed in the brain, liver, and kidney tissues of these animals, respectively, over control animal levels ($p < 0.05$; Fig. 4a). In contrast, a signif-

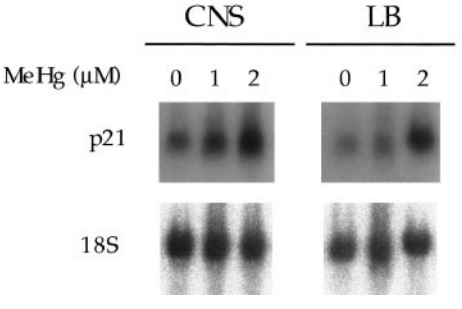


**FIG. 2.** Changes in p21 mRNA levels following MeHg exposure of CNS and LB cell cultures. CNS or LB cells were treated on Day 1 with 0, 1, or 2 $\mu$m MeHg for 24 h, and total RNA was isolated for Northern analysis. The transcript level of 18S rRNA was used to control for equal loading of RNA in each lane. A representative blot is shown.

**TABLE 2**
**Fold Induction of p21 mRNA Expression, in Comparison to GCS–HC Following MeHg Exposure in Primary Embryonic CNS and LB Cells**

| | CNS | | LB | |
|---|---|---|---|---|
| Genes | 1 $\mu$M | 2 $\mu$M | 1 $\mu$M | 2 $\mu$M |
| P21 | 1.5 ± 0.1 | 2.0 ± 0.4* | 1.4 ± 0.3 | 2.6 ± 0.5* |
| GCS-HC | 1.1 ± 0.1 | 1.2 ± 0.1 | 3.9 ± 0.9* | 5.4 ± 0.1* |

*Note.* CNS or LB cells were treated with 0, 1, or 2 $\mu$M MeHg for 24 h and total RNA was isolated for Northern analysis of p21 and GCS-HC expression. The mRNA expression levels were determined by scanning densitometry, normalized to the intensity of the 18S rRNA, and expressed relative to control untreated cells, whose value is set at 1.0. Values shown are the means ± SEM from four independent experiments.

* Significantly different from control cells.

**TABLE 3**

**Relationship Between MeHg, Inorganic Hg Content, and p21 mRNA Expression in the Cortex Region of Female Mice Brain Following MeHg Exposure for 4 Weeks**

| Animal no. | MeHg (ng/g) | Inorganic Hg (ng/g) | Relative p21 mRNA | Blood levels (ng/g) |
|---|---|---|---|---|
| 127 | 111 | NA | 1.0 | NA |
| 154 | 20,757 | 370 | 1.0 | 16,922 |
| 155 | 21,512 | 640 | 4.8 | 16,531 |
| 159 | 22,869 | NA | 4.8 | 15,628 |
| 151 | 26,055 | NA | 6.72 | 15,039 |

*Note.* Animal 127 was one of the unexposed controls. Animals 151, 154, 155, and 159 received 10 ppm MeHg exposure for 4 weeks. MeHg concentration was determined by the cold vapor atomic fluorescence detector. NA, not available.

icantly lower induction was observed for Gadd45, Gadd153 (Ou *et al.*, 1997), and GCS-HC mRNA expression under the same treatment regimen.

*Study B.* By the end of the 4-week exposure period, none of the animals in the 3-ppm group showed either toxicity or induced expression of any examined genes. In the 10-ppm treatment group, four animals appeared to show various signs of toxicity. Tissue MeHg and inorganic Hg analysis at the end of the 4-week period revealed a correlation between MeHg concentrations and p21 mRNA expression levels in the cortex (Table 3). The average MeHg levels in 10-ppm-exposed mice were 22,800 ± 2300 ng/g in cortex and 16,000 ± 800 ng/g in blood. The amount of inorganic Hg was less than 5% of the total Hg in the cortex. A strong elevation of p21 expression was observed in three of 10-ppm-exposed mice that showed signs of toxicity, while the other animal in the same group did not show p21 induction compared to untreated controls. The average increase of p21 mRNA expression in animals who showed p21 induction was 4.5 ± 0.1- and 5.5 ± 0.6-fold elevations in the cerebellum and cortex and 22.7 ± 4.8- and 17.5 ± 5.6-fold elevations in the liver and kidney, compared to those in unexposed animals ($p < 0.05$; Figs. 3 and 4b). We did not observe a significant increase of Gadd45, Gadd153, and GCS-HC mRNA transcript in any of the 10-ppm-exposed animals (Figs. 3 and 4b).

### *Increased p21 Protein Levels Following MeHg Exposure*

We have shown that MeHg exposure results in the up-regulation of p21 mRNA in primary embryonic CNS cells *in vitro* and in adult CNS *in vivo.* To further determine whether the increase in p21 mRNA upon MeHg exposure is accompanied by an increase in protein levels, which ultimately allows p21 to engage in its physiological role in cell cycle, we examined p21 protein levels from control and MeHg-exposed animals. Western blot analysis was intially used to detect p21 protein levels. We repeatedly observed two bands at approximately 21 kDa in the brain, kidney, and liver of adult mouse tissues (Fig. 5a). The upper band represents the 25-kDa IgG light chain dissociated from the IgG holoantibody, which is present in many tissues and may be recognized by the secondary antibody. Further analyses using positive control cell line lysates that expressed only the lower band demonstrated increased p21 protein levels in brain, kidney, and liver tissues of animals with p21 mRNA induction. A representative blot showing the induction of p21 protein expression in the kidney is shown in Fig. 5a. We also confirmed the specificity of the Western blot analysis by performing an immunoprecipitation experiment with an anti-p21 antibody. An IgG control antibody was used to demonstrate the specificity of the immunoprecipitation, since the constant region of the p21 antibody could potentially bind to many proteins cross-reactive with the p21 antibody. The specificity of the p21 signal was demonstrated and increased expression of p21 protein was observed in brain, kidney, and liver

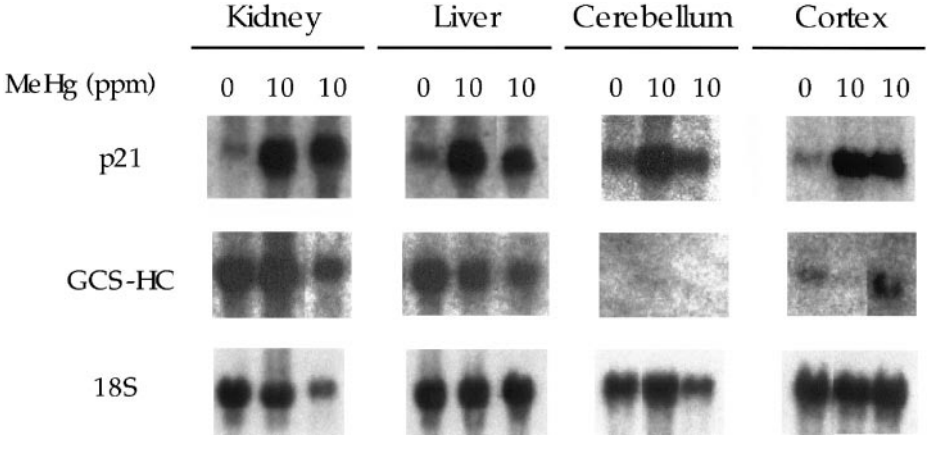


**FIG. 3.** Changes in p21 mRNA levels following MeHg exposure of adult mouse tissues. Female adult mice were exposed to 10 ppm MeHg via drinking water for 4 weeks. This representative blot shows a Northern analysis of expression levels of p21 and GCS-HC mRNA in the cerebellum, cortex, kidney, and liver of control and MeHg-treated animals. The transcript level of 18S rRNA was used to control for equal loading of RNA in each lane.

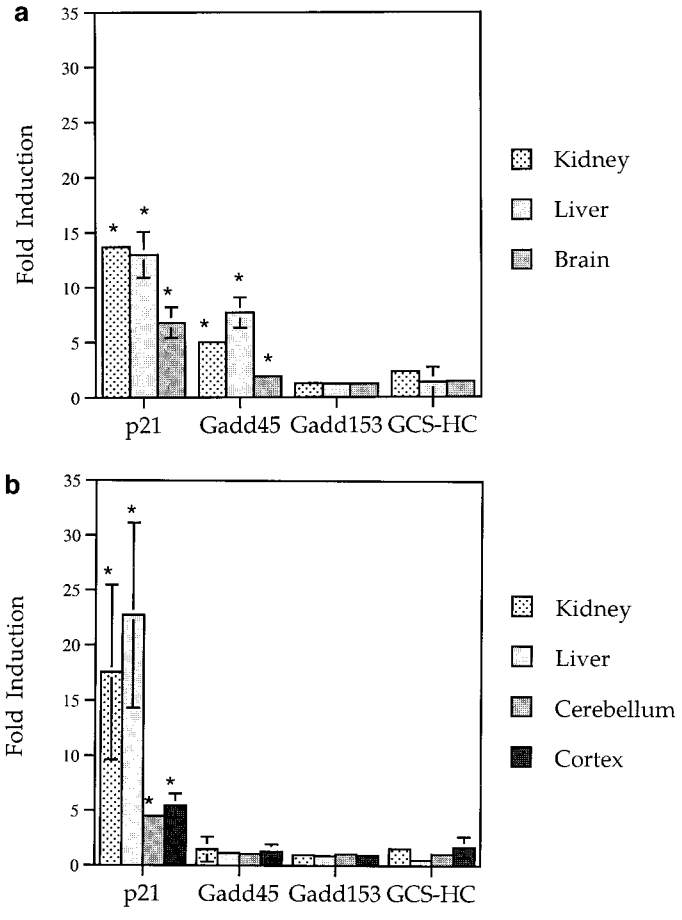


**FIG. 4.** Fold induction of p21 mRNA expression in adult mice following 10 ppm methylmercury exposure for 4 weeks *in vivo.* (a) Study A: Female adult mice were exposed to 10 ppm MeHg through drinking water for 4 weeks. Northern blot analysis and subsequent densitometry scanning were used to quantify relative mRNA levels. The transcript levels are normalized to 18S ribosome message levels and are expressed relative to those in control untreated animals, whose value is set at 1.0. Three of five animals showed symptoms of toxicity accompanied by a strong induction of p21 mRNA expression and, to a lesser degree, Gadd45 and GCS-HC. No induction of Gadd153 was observed. Bars represent the mean of fold induction from three animals ± SD. When no error bars are observed, the SD falls within the plot symbol. (b) Study B: Four animals in the 10-ppm treatment group showed signs of toxicity accompanied by the induction of p21 mRNA expression. There was a limited induction of Gadd45, Gadd153, and GCS-HC. *Significantly different from unexposed controls ($p < 0.05$).

tissues of 10-ppm-exposed animals. A representative blot in the analysis of kidney tissues is shown (Fig. 5b).

## DISCUSSION

The studies presented here demonstrate that MeHg can elicit a dose-dependent activation of p21 in primary embryonic CNS and LB cells *in vitro.* Furthermore, p21 gene expression, correlated with MeHg content *in situ,* is markedly induced at both the mRNA and protein levels in adult tissues (kidney, liver, cerebellum, and cortex) following chronic low dose MeHg exposure *in vivo.* p21 is implicated in the control of cell cycle arrest, and the activation of p21 gene expression observed in our study is consistent with previously described effects of MeHg on cell cycle kinetics (Ponce *et al.,* 1994) and on the inhibition of DNA synthesis (Roy *et al.,* 1991). Together, the observations here support the hypothesis that MeHg compromises normal cell cycle progression at the molecular level in developing embryos.

Pathological examination of *in utero* MeHg-exposed brain tissues from several animal species reveals diffuse cell loss across all brain regions (Reviewed in Burbacher *et al.,* 1990). The observed cell loss may be due either to increased cell death or decreased cell proliferation and cycling upon exposure to MeHg. Subsequent experimental studies on the developing rodent CNS demonstrated inhibitory effects on mitotic activity at brain MeHg concentrations that did not cause overt toxicity (Rodier *et al.,* 1984; Howard and Mottet, 1986). Consistent with previous findings, inhibition of cell cycling appears to be a sensitive gauge of MeHg exposure in primary embryonic CNS cells. By comparing the percentage of viable cells and that of cells undergoing active cell cycling following MeHg exposure, we show that a substantial fraction of observed cell loss can be explained by impaired cell cycling. By comparing the data from colchicine and MeHg-treated cells, the current study further indicates that MeHg-induced cytotoxicity cannot be fully explained by its effects on cell cycling. It is likely that MeHg-induced cytotoxicity occurs via pathways independent of cell cycle inhibition. Cells from p53 and p21 knockout mice may be employed to investigate the relationship between MeHg-induced cytotoxicity and cell cycle inhibition. Further studies should also address whether MeHg-induced altered calcium homeostasis (Hare *et al.,* 1993) and oxidative stress (Yee and Choi, 1994) are ultimately linked to its effect on cell cycling.

The consequences of cell cycle alteration from MeHg exposure may underlie, in part, the vulnerability of the developing CNS to MeHg. In the mature adult CNS, cell cycle arrest may represent a cellular defense mechanism. For example, p53 is thought to maintain genome integrity by initiating a p53-dependent $G_1$ checkpoint arrest, to allow DNA repair or the induction of apoptosis to eliminate the proliferation of genetically damaged cells following genetic insults (Clarke *et al.,* 1993; Kastan *et al.,* 1991; Kuerbitz *et al.,* 1992; Lowe *et al.,* 1993). However, the activation of cell cycle arrest as a result of toxic insults may have a far reaching impact on development. Development of the CNS is a highly temporally and spatially regulated process, and a transient or sustained cell cycle arrest may interfere with the timing of critical developmental windows. This hypothesis is supported by studies showing that p53 wild-type mice capable of initiating cell cycle arrest and apoptosis are more susceptible to agent-induced malformations compared with p53 null mice (Wubah *et al.,* 1996).

The primary effect of MeHg on cell cycle progression is

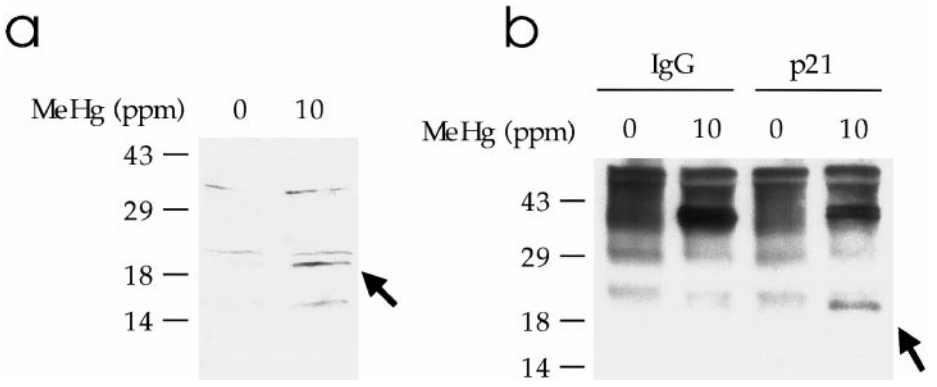


**FIG. 5.** A representative blot showing changes in p21 protein levels following MeHg exposure in adult mouse tissues. Female adult mice were exposed to 10 ppm MeHg via drinking water for 4 weeks. This figure shows a representative blot from the analysis of kidney tissues, which reflects similar changes in p21 protein expression in brain and liver tissues of 10-ppm-exposed animals. (a) Western blot analysis was used to detect the expression of p21 protein levels in the kidney of control and MeHg-exposed animals. (b) Immunoprecipitation followed by Western analysis was used to detect the protein levels in the kidney of control and MeHg-exposed animals. Immunoprecipitates prepared with an antibody against human p21 or rabbit IgG (as indicated above the panel) were separated by SDS–PAGE and immunoblotted with the anti-p21 antibody. For reference, the positions of molecular weight markers (kDa) are shown.

thought to involve a $G_2$–M arrest, via its inhibitory effect on microtubule assembly (Miura *et al.*, 1984; Vogel *et al.*, 1985). However, several lines of evidence also suggest that MeHg may interfere with other components of the cell cycle machinery, such as effects seen in the S and $G_1$ phases (Graff *et al.*, 1993; Ponce *et al.*, 1994; Vogel *et al.*, 1986). For example, using taxol, MeHg effects on microtubule polymerization were reversed while DNA synthesis remained inhibited (Roy *et al.*, 1991). Furthermore, MeHg induced microtubule disassembly was demonstrated using purified microtubules under acute exposure *in vitro* (Miura *et al.*, 1984; Vogel *et al.*, 1985); the biological plausibility of this mechanism remains to be determined. In the present study, we demonstrate the induction of p21 expression following chronic MeHg exposure *in vivo*, a scenario meant to mimic the human exposure profile. We have previously shown that MeHg exposure induces a dose-dependent increase in Gadd45 and Gadd153 mRNA expression in primary embryonic cells (Ou *et al.*, 1997). Although p21 and Gadd45 were first discovered for their association with $G_1$ arrest, evidence regarding their role in $G_2$–M is emerging (Waldman *et al.*, 1996). The induction of genes involved in cell cycle arrest may provide an alternative explanation for the observed cell cycle alterations by MeHg.

In addition to its role in the control of cell cycle progression, p21 has an important function in the terminal differentiation of several cell types. The association of p21 with muscle cell differentiation is supported by the findings in which an increased expression of p21 is associated with MyoD-induced muscle cell differentiation (Halevy *et al.*, 1995). We show that increased expression of p21 is associated with LB but not CNS cell differentiation. Our observations are consistent with several previous findings in which an increased expression of p21 is observed in postmitotic muscle cells, but not in embryonic brain and spinal cord during embryogenesis (Parker *et al.*, 1995), and increased p21 expression is associated with chondrocyte differentiation (Stewart *et al.*, 1997). Our results therefore add to the current literature in support of the hypothesis that p21 is associated with differentiation of some cell types, such as LB, but not others, such as CNS cells.

Despite the differential expression of p21 during the course of CNS and LB differentiation, a similar dose-dependent activation of p21 was observed in both cell types following MeHg exposure. These findings suggest that, while p21 is engaged in the differentiation pathway for certain cell types, induction of p21 and the resulting cell cycle changes in response to MeHg exposure may be a common cellular mechanism.

Comparing the response of several genes to chronic MeHg exposure in adult tissues *in vivo*, we found that p21 is the most responsive gene of all those tested, suggesting that p21 may provide a means for the direct characterization of the effects of MeHg on cell cycling *in vivo*. It is not known yet whether the marked induction of p21 observed in adult CNS resides in neurons or glia. As opposed to embryonic CNS cells, which undergo cell cycling, the adult CNS is composed of postmitotic neurons and other cell types. Glia are one of the major cell types in the adult CNS, and in some regions they outnumber neurons by 10 to 1 (Gordon, 1994). Future studies involving the use of immunocytochemistry and *in situ* hybridization techniques should identify specific cell types associated with p21 induction in the adult CNS. In addition, further studies should address whether MeHg is the ultimate chemical species underlying the induction of p21. Conversion of MeHg to inorganic Hg in the adult CNS *in situ* is shown to be a prominent event following chronic low dose MeHg exposure, and inorganic Hg is implicated as the proximate species for cell number changes of astrocyte and microglia in adult primates (Charleston *et al.*, 1995, 1996). Therefore, in addition to the localization of p21 induction to specific cell types such as neurons or astrocytes, future studies should also involve the

concurrent determination of Hg speciation in order to identify Hg species responsible for the observed p21 induction.

Upstream events and signal transduction pathway leading to the induction of p21 by MeHg remains to be determined. Cell cycle arrest in responding to interferon is mediated through the induction of p21 and is resulted from the activation of transducers and activators of transcription (STAT) proteins (Chin *et al.*, 1996). p21 is identified as a nonenzymatic inhibitor of SAPKs, a subfamily of the MAP kinase (Shim *et al.*, 1996). A likely mechanism for the induction of p21 by MeHg lies in production of oxidative stress. For example, oxidative stress produced by glutathione depletor DEM can activate ERK, a subfamily of the MAP kinase, leading to the induction of p21 (Russo *et al.*, 1995). Oxidative stress-induced p21 may be mediated via the p53 and NF $\kappa$ B pathway. Accumulation of reactive oxygen species can induce a signaling pathway involving tyrosine kinase and NF $\kappa$ B (Anderson *et al.*, 1994). NF $\kappa$ B can further bind to the p53 promoter and regulate the expression of p53 gene (Wu and Lozano, 1994) and possibly activate the p53 downstream molecule, p21. Alternatively, MeHg-induced p21 may be activated by altered calcium concentration. p21 induction has been linked to MAP kinase pathway (Russo *et al.*, 1995) and JNK kinase, a MAP kinase family member, is activated by Pyk2 tyrosine kinase following signals that increase intracellular calcium (Tokiwa *et al.*, 1996).

Our data indicate that cell cycle regulation is an important component of MeHg toxicity in the primary embryonic CNS *in vitro*. In concordance with previous findings (Ou *et al.*, 1997), these results suggest that MeHg-induced cell cycle arrest may be mediated, in part, via the induction of cell cycle regulatory genes. Furthermore, our study provides a methodological framework for the identification of other signaling pathways converging on the induction of cell cycle regulatory genes and cell cycle alteration by MeHg and helps to close an important gap in current understanding of the developmental toxicity of MeHg. The induction of p21 by MeHg reported here should stimulate the search for other cell cycle regulatory molecules contributing to MeHg toxicity *in vivo* and result in improved assessments of risk associated with low level MeHg exposure.

## ACKNOWLEDGMENTS

This work was supported in part by the Center for Ecogenetics and Environmental Health, Grant 5-P30-ES-07033 from the National Institute of Environmental Health Science, NIH, by Grant USEPA R825358 from the Environmental Protection Agency, and by the Consortium for Risk Evaluation with Stakeholder Participation (CRESP) by Department of Energy Cooperative Agreement DE-FCO1-95EW55084. We express sincere appreciation to Dr. Wade Harper for providing the p21 plasmid cDNA. Many thanks to Sungwoo Hong for his assistance in various aspects of this project.

## REFERENCES

Anderson, M. T., Staal, F. J. T., Gitler, C., and Hersenberg, L. A. (1994). Separation of oxidant-initiated and redox-regulated steps in the NF kappa B signal transduction pathway. *Proc. Natl. Acad. Sci. USA* **91,** 11527–11531.

Bartlett, J. D., Luethy, J. D., Carlson, S. G., Sollott, S. J., and Holbrook, N. J. (1992). Calcium ionophore A23187 induces expression of the growth arrest and DNA damage inducible CCAAT/enhancer-binding protein (C/EBP)-related gene, Gadd153. $Ca^{2+}$ increased transcriptional activity and mRNA stability. *J. Biol. Chem.* **267,** 20465–20470.

Burbacher, T. M., Rodier, P. M., and Weiss, B. (1990). Methylmercury developmental neurotoxicity: A comparison of effects in humans and animals. *Neurotoxicol. Teratol.* **12,** 191–202.

Chae, T., Kown, Y. T., Bronson, R., Dikkes, P., Li, E., and Tsai, L. H. (1997). Mice lacking p35, a neuronal specific activator of Cdk5, display cortical lamination defects, seizures, and adult lethality. *Neuron* **18,** 29–42.

Charleston, J. S., Body, R. L., Bolender, R. P., Mottet, N. K., Vahter, M. E., and Burbacher, T. M. (1996). Changes in the number of astrocytes and microglia in the thalamus of the monkey *Macaca fascicularis* following long-term subclinical methylmercury exposure. *NeuroToxicology* **17,** 127–138.

Charleston, J. S., Body, R. L., Mottet, N. K., Vahter, M. E., and Burbacher, T. M. (1995). Autometallographic determination of inorganic mercury distribution in the cortex of the calcarine sulcus of the monkey *Macaca fascicularis* following long-term subclinical exposure to methylmercury and mercuric chloride. *Toxicol. Appl. Pharmacol.* **132,** 325–333.

Chen, Q., Yu, K., Holbrook, N. J., and Stevens, J. L. (1992). Activation of the growth arrest and DNA damage-inducible gene Gadd153 by nephrotoxic cysteine conjugates and dithiothreitol. *J. Biol. Chem.* **267,** 8207–8212.

Chin, Y. E., Kitagawa, M., Su, W. C., You, Z. H., Iwamoto, Y., and Fu, X. Y. (1996). Cell growth arrest and induction of cyclin-dependent kinase inhibitor p21 WAF1/CIP1 mediated by STAT1. *Science* **272,** 719–722.

Choi, B. H., Lapham, L. W., Amin-Zaki, L., and Saleem, T. (1978). Abnormal neuronal migration, deranged cerebral cortical organization, and diffuse white matter astrocytosis of fetal human brain: A major effect of methylmercury poisoning *in utero*. *J. Neuropathol. Exp. Neurol.* **37,** 719–733.

Clarke, A. R., Purdie, C. A., Harrison, D. J., Morris, R. G., Bird, C. C., Hooper, M. L., and Wyllie, A. H. (1993). Thymocyte apoptosis induced by p53-dependent and independent pathways. *Nature* **362,** 849–852.

Clarkson, T. (1991). Methylmercury. *Fundam. Appl. Toxicol.* **16,** 20–21.

el Deiry, W. S., Tokino, T., Velculescu, V. E., Levy, D. B., Parsons, R., Trent, J. M., Lin, D., Mercer, W. E., Kinzler, K. W., and Vogelstein, B. (1993). WAF1, a potential mediator of p53 tumor suppression. *Cell* **75,** 817–825.

Flint, O. P. (1983). A micromass culture method for rat embryonic neural cells. *J. Cell Sci.* **61,** 247–262.

Fornace, A. J. J., Nebert, D. W., Hollander, M. C., Luethy, J. D., Papathanasiou, M., Fargnoli, J., and Holbrook, N. J. (1989). Mammalian genes coordinately regulated by growth arrest signals and DNA-damaging agents. *Mol. Cell Biol.* **9,** 4196–4203.

Gately, D. P., Sharma, M., Christen, R. D., and Howell, S. B. (1996). Cisplatin and taxol activate different signal pathways regulating cellular injury-induced expression of Gadd153. *Br. J. Cancer.* **73,** 18–23.

Gordon, M. S. (1994). Neurons and Glia. In *Neurobiology* (M. S. Gordon, Ed.), pp. 56. Oxford University Press, New York.

Graff, R. D., Philbert, M. A., Lowndes, H. E., and Reuhl, K. R. (1993). The effect of glutathione depletion on methyl mercury-induced microtubule disassembly in cultured embryonal carcinoma cells. *Toxicol. Appl. Pharmacol.* **120,** 20–28.

Halevy, O., Novitch, B. G., Spicer, D. B., Skapek, S. X., Rhee, J., Hannon, G. J., Beach, D., and Lassar, A. B. (1995). Correlation of terminal cell cycle

arrest of skeletal muscle with induction of p21 by MyoD. *Science* **267,** 1018–1021.

Harada, Y. (1977). Congenital Minamata disease. In *Minamata Disease: Methyl Mercury Poisoning in Minamata and Niigata* (R. Tsubak and K. Irukayama, Eds.), pp. 209–239. Kodansha, Tokyo, Japan.

Hare, M. F., McGinnis, K. M., and Atchison, W. D. (1993). Methylmercury increases intracellular concentration of $Ca^{++}$ and heavy metals in NG108–15 cells. *J. Pharmacol. Exp. Ther.* **266,** 1626–1635.

Harper, J. W., Adami, G. R., Wei, N., Keyomarsi, K., and Elledge, S. J. (1993). The p21 Cdk-interacting protein Cip1 is a potent inhibitor of G1 cyclin-dependent kinases. *Cell* **75,** 805–816.

Howard, J. D., and Mottet, N. K. (1986). Effects of methylmercury on the morphogenesis of the rat cerebellum. *Teratology* **34,** 89–95.

Kastan, M. B., Onyekwere, O., Sidransky, D., Vogelstein, B., and Craig, R. W. (1991). Participation of p53 protein in the cellular response to DNA damage. *Cancer Res.* **51,** 6304–6311.

Kuerbitz, S. J., Plunkett, B. S., Walsh, W. V., and Kastan, M. B. (1992). Wild-type p53 is a cell cycle checkpoint determinant following irradiation. *Proc. Natl. Acad. Sci. USA* **89,** 7491–7495.

Lapham, L. W., Cernichiari, E., Cox, C., Myers, G. J., Baggs, R. B., Brewer, R., Shamlaye, C. F., Davidson, P. W., and Clarkson, T. W. (1995). An analysis of autopsy brain tissue from infants prenatally exposed to methylmercury. *NeuroToxicology.* **16,** 689–704.

Li, S., Thompson, S. A., and Woods, J. S. (1996). Localization of gamma-glutamylcysteine synthetase mRNA expression in mouse brain following methylmercury treatment using reverse transcription *in situ* PCR amplification. *Toxicol. Appl. Pharmacol.* **140,** 180–187.

Lowe, S. W., Schmitt, E. M., Smith, S. W., Osborne, B. A., and Jacks, T. (1993). p53 is required for radiation-induced apoptosis in mouse thymocytes. *Nature* **362,** 847–849.

Miller, R. G. (1981). *Simultaneous Statistical Inference.* Springer Verlag, New York.

Miura, K., and Imura, N. (1987). Mechanism of methylmercury cytotoxicity. *Crit. Rev. Toxicol.* **18,** 161–188.

Miura, K., Inokawa, M., and Imura, N. (1984). Effects of methylmercury and some metal ions on microtubule networks in mouse glioma cells and *in vitro* tubulin polymerization. *Toxicol. Appl. Pharmacol.* **73,** 218–231.

Nakayama, K., Ishida, N., Shirane, M., Inomata, A., Inoue, T., Shishido, N., Horii, I., Loh, D. Y., and Nakayama, K. (1996). Mice lacking p21(Kip1) display increased body size, multiple organ hyperplasia, retinal dysplasia, and pituitary tumors. *Cell* **85,** 707–720.

Ormerod, M. G., and Kubbies, M. (1992). Cell cycle analysis of asynchronous cell population by flow cytometry using bromodeoxyuridine label and Hoechst-propidium iodide stain. *Cytometry* **13,** 678–685.

Ou, Y. C., Thompson, S. A., Kirchner, S. C., Kavanagh, T. J., and Faustman, E. M. (1997). Induction of growth arrest and DNA damage-inducible genes Gadd45 and Gadd153 in primary rodent embryonic cells following exposure to methylmercury. *Toxicol. Appl. Pharmacol.* **147,** 31–38.

Parker, S. B., Eichele, G., Zhang, P., Rawls, A., Sands, A. T., Bradley, A., Olson, E. N., Harper, J. W., and Elledge, S. J. (1995). p53-independent expression of p21Cip1 in muscle and other terminally differentiating cells. *Science* **267,** 1024–1027.

Ponce, R. A., Kavanagh, T. J., Mottet, N. K., Whittaker, S. G., and Faustman, E. M. (1994). Effects of methyl mercury on the cell cycle of primary rat CNS cells *in vitro. Toxicol. Appl. Pharmacol.* **127,** 83–90.

Rabinovitch, P. S. (1983). Regulation of human fibroblast growth rate by both noncycling fraction and transition probability is shown by growth in 5-BrdU followed by Hoechst 33258 flow cytometry. *Proc. Natl. Acad. Sci. USA* **80,** 2951–2955.

Ribeiro, P. L., and Faustman, E. M. (1990). Embryonic micromass limb bud and midbrain cultures: Different cell cycle kinetics during differentiation *in vitro. Toxic. In Vitro* **4,** 602–608.

Rodier, P. M., Aschner, M., and Sager, P. R. (1984). Mitotic arrest in the developing CNS after prenatal exposure to methylmercury. *Neurobehav. Toxicol. Teratol.* **6,** 379–385.

Roy, C., Prasad, K. V., Reuhl, K. R., Little, J. E., Valentine, B. K., and Brown, D. L. (1991). Taxol protects the microtubules of concanavalin A-activated lymphocytes from disassembly by methylmercury, but DNA synthesis is still inhibited. *Exp. Cell Res.* **195,** 345–352.

Russo, T., Zambrano, N., Esposito, F., Ammendola, R., Cimino, F., Fiscella, M., Jackman, J., O'Connor, P. M., Anderson, C. W., and Appella, E. (1995). A p53-independent pathway for activation of WAF1/CIP1 expression following oxidative stress. *J. Biol. Chem.* **270,** 29386–29391.

Sager, P. R. (1988). Selectivity of methyl mercury effects on cytoskeleton and mitotic progression in cultured cells. *Toxicol. Appl. Pharmacol.* **94,** 473–486.

Shim, J., Lee, H., Park, J., Kim, H., and Choi, E. J. (1996). A non-enzymatic p21 protein inhibitor of stress-activated protein kinases. *Nature* **381,** 804–806.

Stewart, M. C., Farnum, C. E., and MacLeod, J. N. (1997). Expression of p21 in chondrocyte. *Calcif. Tissue Int.* **61,** 199–204.

Takahashi, T., Nowakowski, R. S., and Caviness, V. S., Jr. (1996). Interkinetic and migratory behavior of a cohort of neocortical neurons arising in the early embryonic murine cerebral wall. *J. Neurosci.* **16,** 5762–5776.

Thompson, S. A. (1996). *Modulation of Glutathione Associated with Methylmercury Exposure in Mice.* Doctoral Dissertation. University of Washington.

Tokiwa, G., Dikic, I., Lev, S., Schlessinger, J. (1996). Activation of Pyk2 by stress signals and coupling with JNK signaling pathway. *Science* **273,** 792–794.

Vogel, D. G., Margolis, R. L., and Mottet, N. K. (1985). The effects of methyl mercury binding to microtubules. *Toxicol. Appl. Pharmacol.* **80,** 473–486.

Vogel, D. G., Robinovitch, P. S., and Mottet, N. K. (1986). Methylmercury effects on cell cycle kinetics. *Cell Tissue Kinet.* **19,** 227–242.

Waga, S., Hannon, G. J., Beach, D., and Stillman, B. (1994). The p21 inhibitor of cyclin-dependent kinases controls DNA replication by interaction with PCNA. *Nature* **369,** 574–578.

Waldman, T., Lengauer, C., Kinzler, K. W., and Vogelstein, B. (1996). Uncoupling of S phase and mitosis induced by anticancer agents in cells lacking p21. *Nature* **381,** 713–716.

Whittaker, S. G., and Faustman, E. M. (1992). Effects of benzimidazole analogs on cultures of differentiating rodent embryonic cells. *Toxicol. Appl. Pharamcol.* **113,** 144–151.

Whittaker, S. G., Wroble, J. T., Silbernagel, S. M., and Faustman, E. M. (1994). Characterization of cytoskeletal and neuronal markers in micromass cultures of rat embryonic midbrain cells. *Cell Biol. Toxicol.* **9,** 359–375.

Woods, J. S., and Ellis, M. E. (1995). Up-regulation of glutathione synthesis in rat kidney by methyl mercury. Relationship to mercury-induced oxidative stress. *Biochem. Pharmacol.* **50,** 1719–1724.

Wu, H., and Lozano, G. (1994). NF-kappa B activation of p53. *J. Biol. Chem.* **269,** 20067–20074.

Wubah, J. A., Ibrahim, M. M., Gao, X., Nguyen, D., Pisano, M. M., and Knudsen, T. B. (1996). Teratogen-induced eye defects mediated by p53-dependent apoptosis [published erratum appears in *Curr. Biol.* **6**(6), 753, 1996]. *Curr. Biol.* **6,** 60–69.

Xiang, H., Hochman, D. W., Saya, H., Fujiwara, T., Schwartzkroin, P. A., and Morrison, R. S. (1996). Evidence for p53-mediated modulation of neuronal viability. *J. Neurosci.* **16,** 6753–6765.

Yee, S., and Choi, B. H. (1994). Methylmercury poisoning induces oxidative stress in the mouse brain. *Exp. Mol. Pathol.* **60,** 188–196.